AJNR

Dynamic Contrast-Enhanced Perfusion MR Imaging Measurements of Endothelial Permeability: Differentiation between Atypical and Typical Meningiomas

Stanley Yang, Meng Law, David Zagzag, Hope H. Wu, Soonmee Cha, John G. Golfinos, Edmond A. Knopp and Glyn Johnson

AJNR Am J Neuroradiol 2003, 24 (8) 1554-1559
http://www.ajnr.org/content/24/8/1554

AJNR Am J Neuroradiol 24:1554–1559, September 2003

Dynamic Contrast-Enhanced Perfusion MR Imaging Measurements of Endothelial Permeability: Differentiation between Atypical and Typical Meningiomas

Stanley Yang, Meng Law, David Zagzag, Hope H. Wu, Soonmee Cha, John G. Golfinos, Edmond A. Knopp, and Glyn Johnson

BACKGROUND AND PURPOSE: **The measurement of relative cerebral blood volume (rCBV) and the volume transfer constant (K^{trans}) by means of dynamic contrast-enhanced (DCE) perfusion MR imaging (pMRI) can be useful in characterizing brain tumors. The purpose of our study was to evaluate the utility of these measurements in differentiating typical meningiomas and atypical meningiomas.**

METHODS: **Fifteen patients with pathologically confirmed typical meningiomas and seven with atypical meningiomas underwent conventional imaging and DCE pMRI before resection. rCBV measurements were calculated by using standard intravascular indicator dilution algorithms. K^{trans} was calculated from the same DCE pMRI data by using a new pharmacokinetic modeling (PM) algorithm. Results were compared with pathologic findings.**

RESULTS: **Mean rCBV was 8.02 ± 4.74 in the 15 typical meningiomas and 10.50 ± 2.1 in the seven atypical meningiomas. K^{trans} was 0.0016 seconds^{-1} ± 0.0012 in the typical group and 0.0066 seconds^{-1} ± 0.0026 in the atypical group. The difference in K^{trans} was statistically significant ($P < .01$, Student t test). Other parameters generated with the PM algorithm (plasma volume, volume of the extravascular extracellular space, and flux rate constant) were not significantly different between the two tumor types.**

CONCLUSION: **DCE pMRI may have a role in the prospective characterization of meningiomas. Specifically, the measurement of K^{trans} is of use in distinguishing atypical meningiomas from typical meningiomas.**

Although meningiomas have readily identifiable imaging features, conventional imaging techniques have not always been reliable in predicting the grade or natural history of tumors (1–4). Studies have shown no statistically significant correlation between histologic features and signal intensity on proton density– or T2-weighted images (5). Sometimes, the aggressiveness of the tumor cannot be accurately characterized, even on the basis of histopathologic findings, partly because of sampling error (6, 7).

Received January 7, 2003; accepted after revision March 17.

From the Departments of Radiology/Division of Neuroradiology (S.Y., M.L., E.A.K., G.J.), Pathology/Division of Neuropathology (D.Z., H.H.W.); and Neurosurgery (J.G.G., E.A.K.), New York University Medical Center, NY; and the Department of Radiology, University of California–San Francisco Medical Center (S.C.).

Supported by NCI/NIH grant R01CA09399.

Address reprint requests to Meng Law, MD, New York University Medical Center, MRI Department, Schwartz Building, Basement HCC, 530 First Avenue, New York, NY 10016.

The World Health Organization (WHO) defines the atypical variant as a meningioma having increased mitotic activity in comparison to the typical meningioma. Other features that can also qualify the lesion as being atypical are increased cellularity and foci of spontaneous or geographic necrosis. More recently, the presence of brain invasion has been described as an important factor in the risk of recurrence (8, 9). The distinction between atypical meningiomas and typical meningiomas is clinically relevant, because benign meningiomas recur in about 7–20% of cases, whereas atypical variants recur in 29–41% (4, 9–11). Furthermore, the aggressiveness of surgical resection and adjunctive radiation therapy is also partly determined by this distinction.

Measurements of the cerebral blood volume (CBV) from dynamic contrast-enhanced (DCE) perfusion MR imaging (pMRI) data have previously been shown to be useful in differentiating gliomas of different grades (12, 13). However, these measurements are based on intravascular indicator dilution

theory (14), which assumes that contrast agent remains intravascular. Because meningiomas lack a true blood-brain barrier, this assumption is violated, and although corrections can be applied, we have noticed that CBV measurements in meningiomas are probably artificially elevated. Therefore, we investigated whether measurements made by using a novel pharmacokinetic modeling (PM) algorithm (15) can help in differentiating typical meningiomas and atypical meningiomas. We hypothesized that atypical meningiomas are associated with a permeability higher than that of typical variants, as expressed by the volume transfer constant (K^{trans}).

Methods

We retrospectively analyzed data collected from patients imaged at our institution from March 1996 to January 2003. This retrospective review of cases was approved by our institutional review board.

Data from 22 patients (four male, 18 female; age range, 27–79 years) were evaluated. In all patients, a histopathologic diagnosis was obtained after near-total or total volumetric resection by two experienced neuropathologists (D.Z., H.H.W.). In 15 patients, meningioma, typical variant (WHO grade I/III), was diagnosed. In seven patients, atypical meningioma (WHO grade II/III) was diagnosed.

Imaging was performed on 1.5-T machines (Siemens AG; Siemens, Erlangen, Germany). Images were acquired by using our standard protocol for the assessment of intracranial lesions. A localizing sagittal T1-weighted image was obtained, followed by nonenhanced axial T1-weighted (TR/TE, 600/14), intermediate-weighted (3400/17), and T2-weighted (3400/119) images. A series of 60 gradient-echo echo-planar images (1000/54) were acquired at 1-second intervals during the first pass of a standard bolus (0.1 mmol/kg) gadopentetate dimeglumine (Magnevist; Berlex, Wayne, NY). The contrast agent was injected at a rate of 5 mL/s, followed by a bolus of sodium chloride solution injected at a rate of 5 mL/s after the 10th baseline acquisition. Six or seven 5-mm-thick sections were acquired. These were positioned from the T2-weighted images to cover the entire tumor.

Image Processing

Data processing was performed offline by using a postprocessing workstation (Sparcstation; Sun Microsystems, Palo Alto, CA) with programs developed inhouse by using the C and IDL programming languages (RSI, Boulder, CO).

Intravascular Indicator Dilution Theory

Relative CBV (rCBV) values were calculated by using standard algorithms based on the intravascular indicator dilution theory (14). The methods for acquiring perfusion data from a set of DCE echo-planar images have been fully described previously (13).

CBVs were measured in regions of interest (ROIs) positioned within the tumor and expressed relative to measurements made in an ROI in the contralateral white matter. ROIs were positioned in areas of maximal abnormality on the basis of color maps. To minimize confounding factors in the rCBV analysis, the size of the ROIs was kept constant (radius, 3.6 mm). Also, measurement of the maximal abnormality, at least in rCBV measurements, has been demonstrated to provide the highest intraobserver and interobserver reproducibility (16).

First-Pass PM

A new algorithm (15) that allows the simultaneous calculation of blood plasma volume (v_p) and K^{trans} was also applied to the dynamic data. The algorithm, first-pass PM, used an exact expression for the concentration of contrast material in the tissue, assuming that contrast exists in the two interchanging compartments (plasma and extravascular extracellular space [EES]). An estimate of the vascular contrast-agent concentration was acquired from normal white matter and fitted to the express for the tissue concentration to derive v_p, K^{trans}, and the volume of the EES (v_e). The flux rate constant ($k_{ep} = K^{trans}/v_e$) was also calculated from the measured K^{trans} and v_e. K^{trans}, v_p, and v_e were measured in the same ROIs in which the rCBV was measured.

Statistical Analysis

The Student *t* test was used to determine whether calculated hemodynamic parameters were significantly different in typical meningiomas and atypical meningiomas. A *P* value of less than .05 was considered to indicate a statistically significant difference, and no correction for multiple comparisons was made.

Results

The Table summarizes the hemodynamic parameters from the series studied. rCBV values ranged from 1.99 to 17.8 in the typical group (n = 15), with a mean of 8.02 ± 4.74. rCBV values in the atypical group (n = 7) ranged from 8.2 to 13.9, with a mean of 10.50 ± 2.1. K^{trans} was 0.0016 seconds^{-1} ± 0.0012 in the typical meningiomas and 0.0066 seconds^{-1} ± 0.0026 in the atypical meningiomas. The difference in K^{trans} was statistically significant ($P < .01$, Student *t* test).

A scatterplot depicting rCBV versus K^{trans} in grade II atypical meningiomas versus grade I typical meningiomas demonstrated good separation in the permeability measure but not in the rCBV (Fig 1).

In the atypical and typical groups, differences in v_p, v_e, and k_{ep} were not statistically significant.

Discussion

The grade of a meningioma has important therapeutic and prognostic implications. Thus, prospectively identifying the histologic grade of a meningioma by using DCE pMRI can be clinically beneficial. In most cases, total surgical resection is planned when it is technically feasible. Preoperatively knowing that one is dealing with a high-grade atypical meningioma can lead to alterations in the planned size, shape, and extent of a craniotomy to ensure clean margins. Preoperative knowledge of an atypical meningioma may also change a neurosurgeon's risk-benefit assessment. In other words, a surgeon may be more aggressive in his or her surgical technique to achieve a complete or Simpson grade I resection (17).

Results of previous studies have shown that the addition of adjuvant radiation therapy improves disease-free survival (18–20). Furthermore, specific parameters regarding the adjuvant dosage have been suggested for the treatment of atypical and malignant grades (21). Therefore, knowing the grade of the

rCBV and K^{trans} data in 22 patients with typical or atypical meningiomas

Patient/Age, y/Sex	rCBV*	K^{trans}, seconds^{-1}†	v_p, %‡	v_e, %§	k_{ep}‖	Location
Typical meningiomas						
1/27/F	9.3	2.1×10^{-3}	0.87	3.06	6.9×10^{-4}	Right temporal
2/33/M	17.8	2.8×10^{-4}	10.94	0.20	1.4×10^{-3}	Left lateral ventricle
3/38/F	14.2	1.8×10^{-3}	9.9	0.19	9.1×10^{-3}	Left frontal
4/41/F	8.7	1.5×10^{-3}	2.79	8.19	1.8×10^{-4}	Left parietal
5/42/F	4.1	1.8×10^{-3}	1.23	1.61	1.2×10^{-3}	Right cerebellopontine
6/42/F	15.8	1.9×10^{-3}	12.3	0.80	2.3×10^{-3}	Right frontal
7/47/F	9.7	0.9×10^{-5}	3.88	1.9×10^{-4}	0.47	Right parasagittal
8/47/F	5.83	1.7×10^{-3}	1.63	0.38	4.5×10^{-3}	Right occipital
9/50/M	4.19	3.0×10^{-3}	5.92	5.36	5.8×10^{-4}	Right frontal
10/51/F	6.54	3.3×10^{-3}	2.63	9.63	3.4×10^{-4}	Right lateral ventricle
11/53/F	1.99	9.3×10^{-5}	8.30	2.3×10^{-2}	4.0×10^{-3}	Left parietal
12/55/M	2.15	2.7×10^{-4}	2.11	5.7×10^{-2}	4.7×10^{-3}	Left parafalcine
13/56/F	7.5	3.5×10^{-3}	2.56	7.56	4.6×10^{-4}	Left sphenoid wing
14/57/F	6.94	2.1×10^{-3}	2.47	8.09	2.6×10^{-4}	Left frontal
15/59/M	5.59	2.0×10^{-4}	6.78	3.5×10^{-2}	5.7×10^{-3}	Right parafalcine
Mean	8.02	1.6×10^{-3}	4.95	3.01	3.4×10^{-2}	Not applicable
SD	4.74	1.2×10^{-3}	3.80	3.66	1.2×10^{-1}	Not applicable
Atypical meningiomas						
16/46/F	8.97	1.1×10^{-2}	1.57	13.7	8.2×10^{-4}	Right parafalcine
17/49/F	8.2	6.3×10^{-3}	3.09	5.17	1.2×10^{-3}	Left parasagittal
18/52/F	11.4	8.2×10^{-3}	9.80	36.5	2.2×10^{-4}	Left frontal
19/58/F	12.07	7.1×10^{-3}	12.02	32.2	2.2×10^{-4}	Right parietal
20/58/F	10.45	3.2×10^{-3}	12.3	1.44	2.2×10^{-3}	Left frontal
21/69/F	8.52	4.6×10^{-3}	2.78	1.68	2.7×10^{-3}	Right temporal
22/79/F	13.9	5.6×10^{-3}	3.58	11.49	4.9×10^{-4}	Right frontal
Mean	10.50	6.6×10^{-3}	6.45	14.6	1.1×10^{-3}	Not applicable
SD	2.1	2.59×10^{-3}	4.71	14.3	9.9×10^{-4}	Not applicable

* $P = .10$.
† $P = .002$.
‡ $P = .48$.
§ $P = .08$.
‖ $P = .31$.

tumor before treatment helps in planning the resection planning and the dose of adjuvant radiation. Histopathologic differentiation is based on the WHO definition, which describes the atypical variant of meningioma as having increased mitotic activity, as well as increased cellularity, foci of spontaneous or geographic necrosis and brain invasion (Fig 2). However, the histopathologic diagnosis may not be as clear cut. On these and other occasions, findings of increased permeability or perfusion can provide the clinician with additional information for determining further neuro-oncologic treatment.

At our institution, the recommendation of the neurosurgeons and neuro-oncologists for the treatment of atypical meningiomas includes follow-up MR imaging every 3 months for the first 12 months, followed

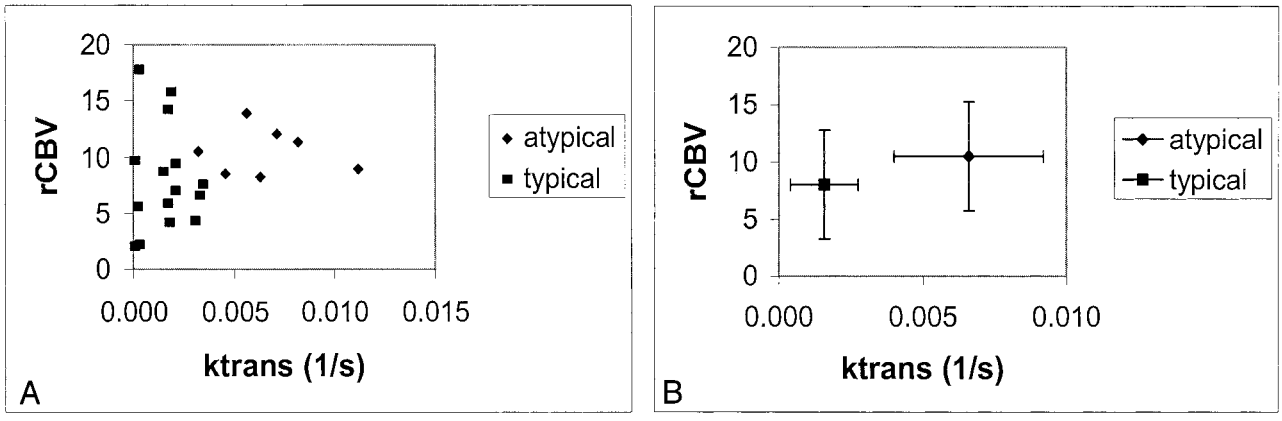

FIG 1. Scatterplots of rCBV versus K^{trans}.
A, Grade II (*diamonds*) versus grade I (*squares*) meningiomas. The groups are well separated in the permeability measure but not in rCBV.
B, rCBV versus K^{trans} for the two grades. Data points are the mean values. Error bars indicate the SD.

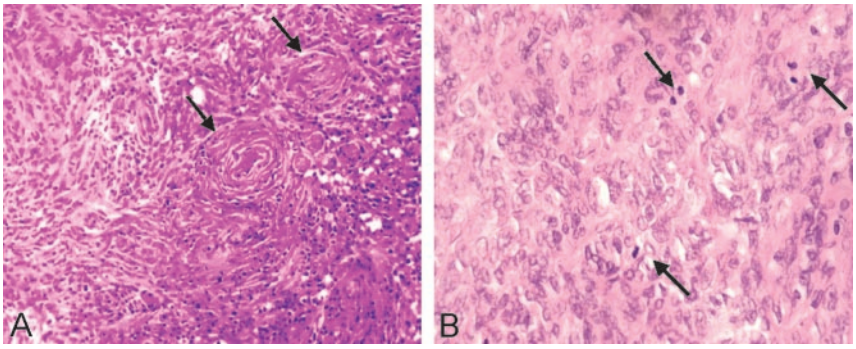

FIG 2. Photomicrographs (hematoxylin-eosin).

A, Medium-power image demonstrates tumor cells, which form a lobulated pattern with whorls (*arrows*) in a typical meningioma (original magnification ×100).

B, High-power images demonstrates at least three mitotic figures (*arrows*) in this atypical meningioma (original magnification ×200).

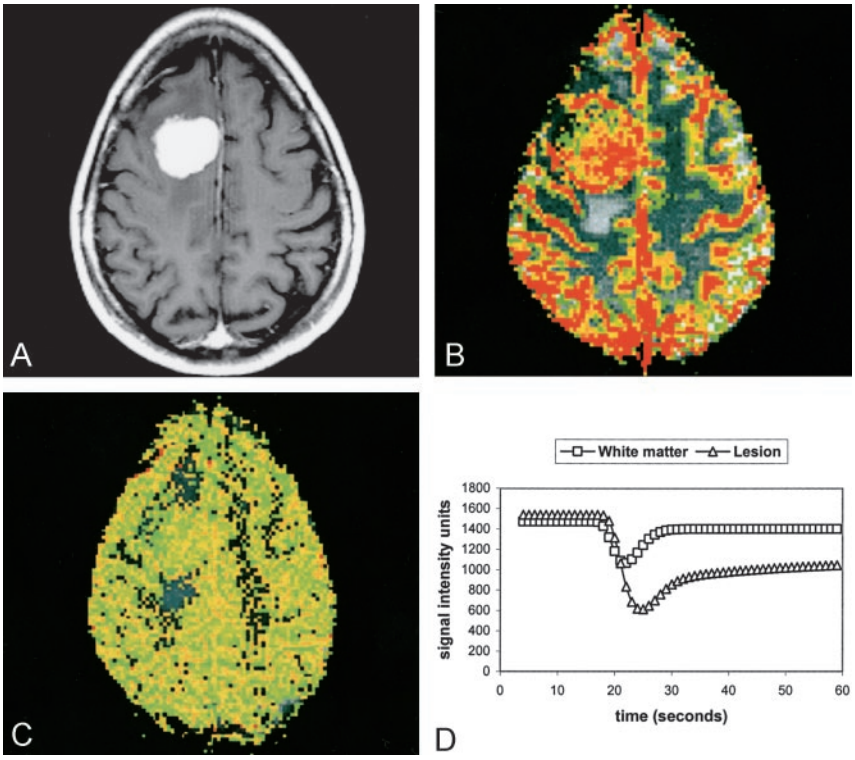

FIG 3. Pathologically confirmed meningioma (WHO grade I/III).

A, Axial contrast-enhanced T1-weighted (600/14) MR image.

B, Axial gradient-echo (1000/54) pMRI image with an rCBV color overlay demonstrates high rCBV throughout the lesion.

C, Axial gradient-echo (1000/54) axial pMRI image with SD25 depicts a decrease in signal intensity after 25 seconds.

D, Normalized signal intensity plotted against time for the white matter (*squares*) and the lesion (*triangles*). The *lines* represent the fitted curves derived by using the first-pass PM algorithm. The return to baseline is more rapid in typical meningiomas than in atypical meningiomas.

by yearly MR imaging thereafter. Patients with atypical meningiomas are also considered for external-beam irradiation after resection, regardless of the presence of residual tumor. The dura is thought to be globally abnormal in patients with atypical meningiomas. In patients with recurrent atypical tumors, gamma-knife radiosurgery is sometimes recommended.

Previous attempts to prospectively assess the grade of a tumor by using DCE pMRI to measure rCBV were not successful. Notably, Zhu et al (22) found no correlation between rCBV and tumor grade in two malignant and 12 benign meningiomas. In our series of seven atypical and 15 benign meningiomas, this was also the case.

However, a few reports describe the quantitative assessment of vascular permeability in the characterization of meningiomas. Uematsu et al (23), demonstrated the use of T1- and T2*-shortening effects to estimate permeability and vascularity in meningiomas and acoustic neurinomas. Although no comparison with atypical meningiomas was made, the investigators found lower permeability in the typical meningioma group than in the neurinoma group. This finding is consistent with the results of our comparison of typical and atypical meningiomas (Figs 3 and 4).

The first-pass PM algorithm used in this study has a number of potential advantages over alternative PM algorithms (24). First, most PM algorithms are applied to data during the washout of contrast material when the plasma concentration is low. Taken with the relatively low vascularity of the brain, this approach prevents an accurate assessment of blood (or plasma) volume. The first-pass PM algorithm used data acquired during the first pass when the concentration of contrast material is high. Therefore, as far as we know, first-pass PM is the only algorithm that provides simultaneous estimates of the blood volume, the transfer constant, and the volume of the EES. Second, most PM methods require the acquisition of data over tens of minutes to adequately sample the washout curve. The first-pass PM algorithm requires only first-pass data, which can be acquired in 1 minute or less. Finally, the algorithm uses image data acquired with susceptibility-weighted echo-planar imaging, and

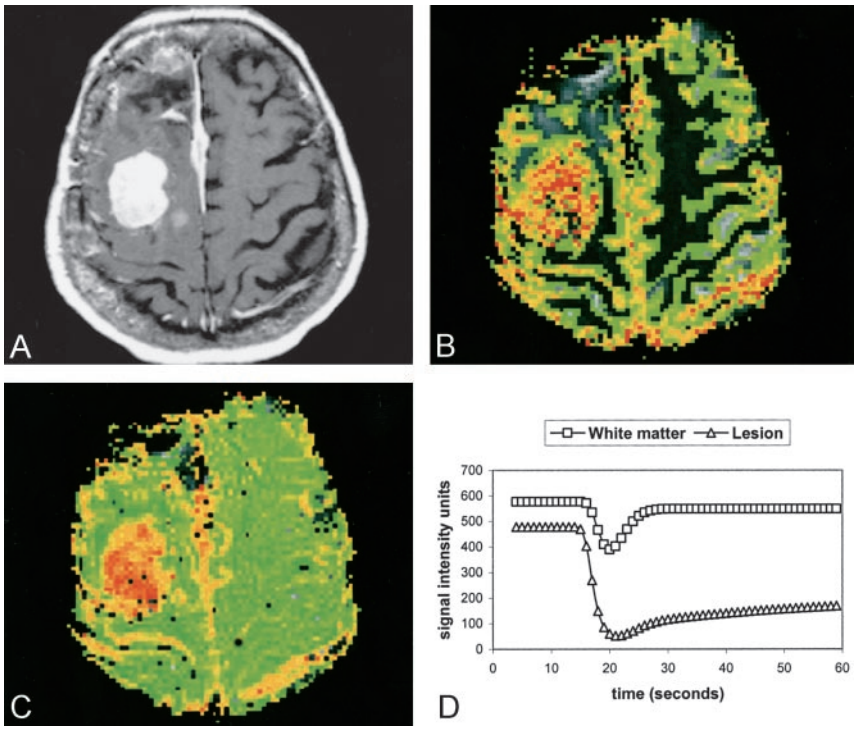

FIG 4. Pathologically confirmed atypical meningioma (WHO grade II/III).

A, Axial contrast-enhanced T1-weighted (600/14) MR image.

B, Axial gradient-echo (1000/54) pMRI with an rCBV color overlay demonstrates high rCBV throughout the lesion.

C, Axial gradient-echo (1000/54) pMRI with an SD25 overlay. *Red* indicates regions of greatest decrease in signal intensity, which are correlated to areas of increased permeability. Qualitatively, this is the best way to distinguish this lesion from that shown in Figure 2.

D, Normalized signal intensity plotted against time for the white matter (*squares*) and the lesion (*triangles*). The *lines* represent the fitted curve derived by using the first-pass PM algorithm. Increased permeability results in a slower return to baseline.

thus, it can sample as many as about 10 sections with 1-second temporal resolution. Methods such as that of Uematsu et al (23), which involve a combination of T1 and T2* weighting, acquire data more slowly; therefore, they are restricted to single-section acquisitions. T1 effects may have a small impact, even on a first-pass T2*-weighted acquisition. The result is underestimation of the decrease in signal intensity. Currently, we use a 30° flip angle in our protocol to counter this effect.

The finding that K^{trans} is elevated in atypical meningiomas may reflect their histopathologic characteristics. The relationship of the capillary ultrastructure to the grade of the tumor has not been fully established in meningiomas (25, 26), but the existing literature regarding gliomas suggests that capillary leakiness and the size of endothelial gap junctions are positively correlated with the grade (27–29). One feature often associated with atypical meningiomas, and one possibly related to increased capillary leakiness, is micronecrosis. This micronecrosis is described as spontaneous or geographic necrosis in the WHO model (2). In their study of atypical and malignant meningiomas, McLean et al (3) reported the survival statistics of patients with benign, atypical, or malignant meningiomas. They related the presence of micronecrosis, a feature more prevalent in atypical meningiomas than in typical ones, with the risk of recurrence as well as survival. At 36 months, 32% in patients with micronecrosis survived, and 71% of those without micronecrosis survived. The degree of vascular permeability may possibly be related to the degree of micronecrosis in a meningioma. The lack of correlation between tumor grade and k_{ep} suggests that the rate of transfer from the intravascular space to the extravascular space is the important element to the equation, rather than the absolute indices of the leakage of contrast material. Naturally, such key parameters are not accessible with conventional imaging, and this limitation may further account for why atypical variants are virtually indistinguishable on conventional contrast-enhanced T1-weighted images.

Conclusion

Our data show that an analysis of the dynamic perfusion curves generated by using echo-planar contrast-enhanced T2*-weighted sequences with respect to the permeability between intravascular and extravascular compartments can provide additional information for the preoperative assessment of intracranial meningiomas. This information can be of clinical benefit. We demonstrate good correlation between K^{trans} and the histologic grade of the meningiomas. Pathologically, the K^{trans} measurement may be related to the degree of micronecrosis. Because the atypical and typical variants of meningioma have different recurrence rates, K^{trans} provides one of the few prospective measures of tumor behavior and prognosis. The role of brain invasion in atypical meningiomas, which is known to change the prognosis and treatment, has not been fully explored. The measurement of perfusion parameters in the brain adjacent to meningiomas and their correlation to brain invasion provide an interesting area for future study, and in fact, this project is currently in progress at our institution. Further prospective investigation in a larger cohort of patients with meningiomas is needed, although this work is hindered by the relatively low incidence of atypical or even malignant variants. Intraobserver and interobserver validation studies

should be performed to demonstrate the reliability and reproducibility of these advanced techniques.

References

1. Jellinger K, Slowik F. **Histological subtypes and prognostic problems in meningiomas**. *J Neurol* 1975;208:279–298
2. Kleihues P, Cavenee WK ed. *Pathology and Genetics of Tumours of the Nervous System.* Lyon, France: IARC Press; 2000
3. McLean CA, Jolley D, Cukier E, et al. **Atypical and malignant meningiomas: importance of micronecrosis as a prognostic indicator**. *Histopathology* 1993;23:349–353
4. Mahmood A, Caccamo DV, Tomecek FJ, et al. **Atypical and malignant meningiomas: a clinicopathological review**. *Neurosurgery* 1993;33:955–963
5. Carpeggiani P, Crisi G, Trevisan C. **MRI of intracranial meningiomas: correlations with histology and physical consistency**. *Neuroradiology* 1993;35:532–536
6. Brainard JA, Prayson RA, Barnett GH. **Frozen section evaluation of stereotactic brain biopsies: diagnostic yield at the stereotactic target position in 188 cases**. *Arch Pathol Lab Med* 1997;121:481–484
7. Hall WA. **The safety and efficacy of stereotactic biopsy for intracranial lesions**. *Cancer* 1998;82:1749–1755
8. Perry A, Scheithauer BW, Stafford SL, et al. **"Malignancy" in meningiomas: a clinicopathologic study of 116 patients, with grading implications**. *Cancer* 1999;85:2046–2056
9. Perry A, Stafford SL, Scheithauer BW, et al. **Meningioma grading: an analysis of histologic parameters**. *Am J Surg Pathol* 1997;21:1455–1465
10. Maier H, Ofner D, Hittmair A, et al. **Classic, atypical, and anaplastic meningioma: three histopathological subtypes of clinical relevance**. *J Neurosurg* 1992;77:616–623
11. Kolles H, Niedermayer I, Schmitt C, et al. **Triple approach for diagnosis and grading of meningiomas: histology, morphometry of Ki-67/Feulgen stainings, and cytogenetics**. *Acta Neurochir* 1995;137:174–181
12. Aronen HJ, Gazit IE, Louis DN, et al. **Cerebral blood volume maps of gliomas: comparison with tumor grade and histologic findings**. *Radiology* 1994;191:41–51
13. Knopp EA, Cha S, Johnson G, et al. **Glial neoplasms: dynamic contrast-enhanced T2*-weighted MR imaging**. *Radiology* 1999;211:791–798
14. Rosen BR, Belliveau JW, Vevea JM, et al. **Perfusion imaging with NMR contrast agents**. *Magn Res Med* 1990;14:249–265
15. Johnson G, Wetzel S, Cha S, et al. **Simultaneous measurement of blood volume and vascular transfer constant by first pass pharmacokinetic modeling**. In: *Proceedings of the International Society for Magnetic Resonance in Medicine.* Berkeley, CA: International Society for Magnetic Resonance in Medicine; 2002
16. Wetzel SG, Cha S, Johnson G, et al. **Relative cerebral blood volume measurements in intracranial mass lesions: interobserver and intraobserver reproducibility study**. *Radiology* 2002;224:797–803
17. Wilson CB. **Meningiomas: genetics, malignancy, and the role of radiation in induction and treatment: the Richard C. Schneider Lecture.** *J Neurosurg* 1994;81:666–675
18. Miralbell R, Linggood RM, de la Monte S, et al. **The role of radiotherapy in the treatment of subtotally resected benign meningiomas**. *J Neurooncol* 1992;13:157–164
19. Barbaro NM, Gutin PH, Wilson CB, et al. **Radiation therapy in the treatment of partially resected meningiomas**. *Neurosurgery* 1987;20:525–528
20. Taylor BW, Jr., Marcus RB, Jr., Friedman WA, et al. **The meningioma controversy: postoperative radiation therapy**. *Int J Radiat Oncol Biol Phys* 1988;15:299–304
21. Milosevic MF, Frost PJ, Laperriere NJ, et al. **Radiotherapy for atypical or malignant intracranial meningioma**. *Int J Radiat Oncol Biol Phys* 1996;34:817–822
22. Zhu F, Zhou Y, Wang C, et al. **Perfusion MRI evaluation of correlating perfusion constants with histologic findings in meningiomas**. In: *Proceedings of the International Society for Magnetic Resonance in Medicine.* Berkeley, CA: International Society for Magnetic Resonance in Medicine; 2002
23. Uematsu H, Maeda M, Sadato N, et al. **Vascular permeability: quantitative measurement with double-echo dynamic MR imaging–theory and clinical application**. *Radiology* 2000;214:912–917
24. Tofts PS. **Modeling tracer kinetics in dynamic Gd-DTPA MR imaging**. *J Magn Reson Imaging* 1997;7:91–101
25. Ikushima I, Korogi Y, Kuratsu J, et al. **Dynamic MRI of meningiomas and schwannomas: is differential diagnosis possible?** *Neuroradiology* 1997;39:633–638
26. Long DM. **Vascular ultrastructure in human meningiomas and schwannomas**. *J Neurosurg* 1973;38:409–419
27. Dvorak HF, Nagy JA, Feng D, et al. **Vascular permeability factor/vascular endothelial growth factor and the significance of microvascular hyperpermeability in angiogenesis**. *Curr Top Microbiol Immunol* 1999;237:97–132
28. Provenzale JM, Wang GR, Brenner T, et al. **Comparison of permeability in high-grade and low-grade brain tumors using dynamic susceptibility contrast MR imaging**. *AJR Am J Roentgenol* 2002;178:711–716
29. Roberts HC, Roberts TP, Brasch RC, et al. **Quantitative measurement of microvascular permeability in human brain tumors achieved using dynamic contrast-enhanced MR imaging: correlation with histologic grade**. *AJNR Am J Neuroradiol* 2000;21:891–899